

Performance of L-493 Macro porous Resin for Adsorption of Trihalomethanes from Water

Shaogang Liu · Wanting Huang · Wei Shu ·
Zhangyan Li · Bernard A. Goodman · Xuecai Tan ·
Kaisheng Diao 

Received: 10 March 2018 / Accepted: 26 June 2018 / Published online: 5 July 2018
© Springer International Publishing AG, part of Springer Nature 2018

Abstract The commercial resin Dowex Optipore L-493 was evaluated for the removal of the trihalomethanes (THMs) from water. Adsorption amounts were in the order $\text{CHBr}_3 \approx \text{CHBr}_2\text{Cl} > \text{CHBrCl}_2 > \text{CHCl}_3$, insensitive to pH in the range 3.0–7.0, but decreased at pH higher values. They were little affected by the presence of co-existing anions and humic acid, and environmental impurities in a spiked natural water sample were only slightly lower than those obtained with pure water. In a comparison with several other commercial adsorbents, the overall performance of L-493 for adsorption of THMs was comparable with the best of those tested, and superior to IR 120, IRC 748, and powder activated carbon. THM adsorption on L-493 was endothermic, and fitted by the pseudo-second-order kinetic and

Langmuir isotherm models; maximum adsorption was 228.6, 247.3, 250.6, and 253.7 $\mu\text{g/g}$, for CHCl_3 , CHBrCl_2 , CHBr_2Cl , and CHBr_3 , respectively. Charge distributions and dipole moments were calculated for the optimized structures using the hybrid density functional theory (DFT) method. Both hydrophobic effects and electrostatic interactions play important roles in the adsorption process. The L-493 resin was easily regenerated and could be recycled using 0.1 M NaOH, with only a small decrease in its initial adsorption capacities. Overall, this research shows that L-493 is potentially a valuable adsorbent for the removal of THMs during water treatment.

Keywords L-493 resin · Trihalomethanes · Density functional theory · Adsorption mechanism · Drinking water

Electronic supplementary material The online version of this article (<https://doi.org/10.1007/s11270-018-3898-7>) contains supplementary material, which is available to authorized users.

S. Liu · W. Huang · Z. Li · X. Tan · K. Diao (✉)
Guangxi Colleges and Universities Key Laboratory of Food Safety and Pharmaceutical Analytical Chemistry, Guangxi Key Laboratory of Chemistry and Engineering of Forest Products, School of Chemistry and Chemical Engineering, Guangxi University for Nationalities, Nanning 530008 Guangxi, China
e-mail: Diaokaisheng2010@163.com

W. Shu
Department of Cell Biology and Genetics, Guangxi Medical University, Nanning 530021 Guangxi, China

B. A. Goodman
College of Physical Science and Engineering, Guangxi University, Nanning 530004 Guangxi, China

1 Introduction

Disinfection by-products (DBPs) are formed by reactions between disinfectants (e.g., free chlorine, chloramines, etc.) and natural organic matter present in drinking water supplies. Trihalomethanes (THMs) are one of the most hazardous groups of DBPs formed in drinking water and have received much attention because of their potentially carcinogenic properties (Bull et al. 1995). The combined contents of the THMs generated during water disinfection, namely chloroform (CHCl_3), dichlorobromomethane (CHBrCl_2), dibromochloromethane (CHBr_2Cl), and bromoform (CHBr_3), are regulated in drinking water to a maximum total contaminant level of 80 $\mu\text{g/L}$ under Stage I

of the Disinfectant/Disinfection Byproducts Rule (USEPA 1998). Therefore, great efforts are being made to develop innovative and cost-effective methods for the removal of THMs from drinking water.

Various techniques, such as adsorption (Lu et al. 2005), ozonation (Chiang et al. 2009), and membrane filtration (Uyak et al. 2008), have been used to remove the DBPs from drinking water. Among these, adsorption has an advantage of low cost and high efficiency, and a wide range of materials have been investigated for the removal of THMs from water. These include the use of natural or engineered adsorbents, such as soils, activated carbon (Lu et al. 2005, 2006; Babi et al. 2007), siliceous materials (Prarat et al. 2011; Prarat et al. 2013), and polymeric resins (Wang et al. 2014). Activated carbon has traditionally been the most common adsorbent used in water purification, but recently polymeric resins have become an increasingly popular alternative because of their low cost, high porosity, large surface area, ease of regeneration, and high adsorption capacity. Many resins with hypercrosslinked, aminated macroporous, microporous, or magnetic structures have now been synthesized and applied to water purification (Pan et al. 2008; Pan et al. 2005; Wang et al. 2014). Among these, Dowex Optipore L-493, which is a commercially available polystyrene crosslinked with divinylbenzene, has been developed as an adsorbent material for industrial applications, including the removal of acrylonitrile (Wegmann et al. 2011) and heavy metals (e.g., copper, lead, iron) from water (Yıldız et al. 2011). However, to the best of our knowledge, there is little information available on the effectiveness of L-493 for adsorbing THMs from drinking water.

In the present work, we have systematically investigated the mechanism and predominant factors that control THMs adsorption on L-493 resin. These include the influence of adsorbent dosage, solution pH, contact time, and temperature. Thermodynamic parameters, such as the standard Gibbs energy change (ΔG°), enthalpy change (ΔH°), and entropy change (ΔS°), were calculated. Additionally, the performances of several other commercial adsorbents for THMs adsorption were compared with that of L-493. Finally, quantum mechanical calculations were performed to provide a theoretical foundation for further understanding the adsorption of THMs on L-493.

2 Materials and Methods

2.1 Materials

The THMs, CHCl_3 , CHBrCl_2 , CHBr_2Cl , and CHBr_3 were all obtained from J&K Science Co., Ltd., Beijing. Dowex Optipore L-493 manufactured by Dow Chemical (Midland, MI, USA) was purchased from Sigma-Aldrich Company (St. Louis, MO, USA). Amberlite IR 120, XAD-4, and XAD-1180 were purchased from Acros Organics (New Jersey, USA), and Amberlite® IRC 748 from Alfa Aesar (Ward Hill, MA, USA). Powder activated carbon (PAC) was purchased from Tianjin Guangfu Chemical Reagent Co. Ltd. (Tianjin, China). Except for L-493, the main physicochemical properties of the adsorbents used in this study are presented in Table S1 Supporting information. Other chemicals were of the highest purity available, and were supplied by Sinopharm Chemical Reagent Beijing Co., Ltd. (Beijing, China). Humic acid (HA) was purchased from Aldrich Chemical Company, USA. A natural water sample was collected from the Yongjiang river in Nanning city, Guangxi, China. All solutions were prepared with ultrapure water produced by a Milli-Q system (Advanatge A10, Millopore, Billerica, MA, USA).

2.2 Pretreatment of the Resins

Prior to use, all resins were washed with distilled water, then rinsed with 1.0 M NaOH solution, and finally washed repeatedly with distilled water until pH 6.0–7.0. Finally, the resins were extracted with ethanol for 8 h in a Soxhlet apparatus, and dried in a vacuum desiccator at 50 °C for 2 h.

2.3 Characterization of L-493 Resin

The chemical composition and structure of L-493 were determined by elemental analysis (EA, Elemental Vario MICRO) and Fourier transform infrared (FT-IR) spectroscopy (Thermo Nicolet Co., USA), and its surface morphology by field emission scanning electron microscopy (FE-SEM, SUPRA 55, Carl Zeiss AG). The BET specific surface area and pore size distribution of L-493 were determined by N_2 adsorption–desorption isotherms using an automatic surface analyzer (ASAP2020, Micromeritics Instrument, USA). Its thermal stability was tested by thermogravimetric analysis (TGA) of solid samples, using a TGA Q50 simultaneous

thermal analyzer (Waters, USA), heated from 35 to 700 °C at a heating rate of 10 °C/min under a N₂ flow rate of 100 mL/min. Zeta potentials were measured in a Zetasizer 2000 Analyzer (Malvern, Mastersizer 2000 Instruments Co., USA).

2.4 Batch Adsorption Experiment

The adsorbent L-493 (40 mg) and THMs stock solution (0.4 mL, 20 mg/L) were added to a series of conical flasks (each containing 40 mL of ultrapure water) and the ionic strength was fixed at 1 mM using NaCl. All experiments were performed at pH 7.0 in 5 mM phosphate buffer unless otherwise stated. For other solutions, the pH was adjusted with 0.1 mol/L HCl or NaOH, and the flasks shaken at 150 rpm and 25 °C for 24 h. The effects of solution pH, ionic strength, co-existing anions (i.e., Cl⁻, NO₃⁻, CO₃²⁻, SO₄²⁻ and PO₄³⁻) as Na⁺ salts and HA were investigated via batch experiments at 25 °C with 1.0 g/L dosage of L-493. The adsorption properties of L-493 were compared with those of four other resins (Amberlite IR 120, Amberlite XAD-4, Amberlite XAD-1180 and Amberlite IRC 748) and PAC. In addition, kinetic information was obtained by varying the equilibration time between 0 and 24 h for an initial concentration of THMs of 200 µg/L. Adsorption isotherms were measured for various initial concentrations of CHCl₃, CHBrCl₂, CHBr₂Cl, and CHBr₃ from 0 to 200 µg/L in single and mixed systems. The experimental temperatures were controlled at 15, 25 and 35 °C. Selective adsorption was also investigated using a mixed solute containing the same concentrations of the four THMs. To investigate the adsorption performance for THMs by L-493 with natural waters, 200 µg/L THMs was spiked into water collected from the Yongjiang river at Nanning; its major quality parameters are summarized in Table S2.

The amount of THMs adsorbed by L-493 and the removal efficiency were calculated as follows:

$$q_t = \frac{(C_0 - C_t)V}{m} \quad (1)$$

$$\text{THM removal efficiency}\% = \frac{C_0 - C_t}{C_0} \times 100\% \quad (2)$$

where C_0 and C_t (µg/L) are the concentrations of THMs in aqueous solution initially and at time t (h), respectively; q_t (µg/g) is the amount of THMs adsorbed at

equilibrium, V is the volume of THMs solution (L), m is the mass of adsorbent (g). All experiments were performed in duplicate.

2.5 Analytical Methods

After reaching equilibrium, the 30 mL supernatant solution was extracted with *t*-methyl *t*-butyl ether according to the USEPA method 551.1 (USEPA Method 551.1 1990). THMs concentrations were determined by a gas chromatograph equipped with an electron capture detector (GC/ECD, Agilent GC6890) and a fused silica capillary column (HP-5, 30 m × 0.32 mm i.d. × 0.25 µm film thickness). The GC-ECD was operated at an injection temperature of 180 °C, detector temperature of 272 °C and oven temperature of 110 °C.

2.6 Desorption and Regeneration

In order to better understand the mechanism of THMs adsorption on L-493, desorption experiments were performed in batch experiments with 40 mg L-493 pretreated with 40 mL THMs solution (200 µg/L, pH 7.0) using 0.1 M NaOH, 0.1 M HCl, ethanol/H₂O ($v:v = 1:1$) as desorbing agent. Consecutive adsorption–desorption cycles were repeated five times to establish the re-usability of the L-493.

2.7 Computational Details

All calculations used the Gaussian 09 software package. The ground state geometries and electronic structures of THMs were optimized by using the hybrid density functional theory (DFT) method, using periodic boundary conditions at the B3LYP level of theory with the 6–311**G (d,p) set performed on Gaussian 09 program package (Frisch et al. Gaussian, Inc., Wallingford, CT 2010). For molecules which have more than one possible conformation, the conformation with the lowest electronic energy was identified and adopted for the calculations. Frequency calculations were computed on these geometries at the same level to verify that they are real minima on the potential energy surface without any imaginary frequency. All calculations were confirmed by frequency analysis that the ground state configuration and zero-point correction value was obtained.

3 Results and Discussion

3.1 Characterization of L-493

Measurements of the morphology of L-493 by SEM (Fig. 1a and insert) showed that the sample consists of spherical beads with particle diameters approximately 0.3 to 0.85 mm. The FTIR spectrum has bands at 900–700 cm^{-1} , which can be assigned to the superposition of mono- and disubstituted benzenes in poly (styrene-co-divinylbenzene). The peak at 820 cm^{-1} is attributed to the 1,4-disubstituted benzene ring, and those at 1450 and 2925 cm^{-1} are assigned to $-\text{CH}_3$ and $-\text{CH}_2-$ stretching vibrations (Fig. 1b). Elemental analysis gave C, H, S, and N

contents of 84.79%, 6.98%, 2.25 and 0.156%, respectively. The N_2 adsorption–desorption curves show an adsorption isotherm consistent with a macroporous structure according to the international Union of Pure and Applied Chemistry (IUPAC) classification. The BET surface area of 823.5 m^2/g is less than the value of 1100 m^2/g quoted by the Dow Chemical Company (<https://www.sigmaaldrich.com/catalog/product/sial/573698?lang=zh®ion=CN> last accessed, February 2018). The mean pore diameter and total pore volume were 5.7 nm and 0.33 cm^3/g , respectively. Thermogravimetric analysis indicated that degradation of L-493 commenced at about 150 $^\circ\text{C}$ and was complete by 600 $^\circ\text{C}$. Thus, it is sufficiently stable for use in water treatment.

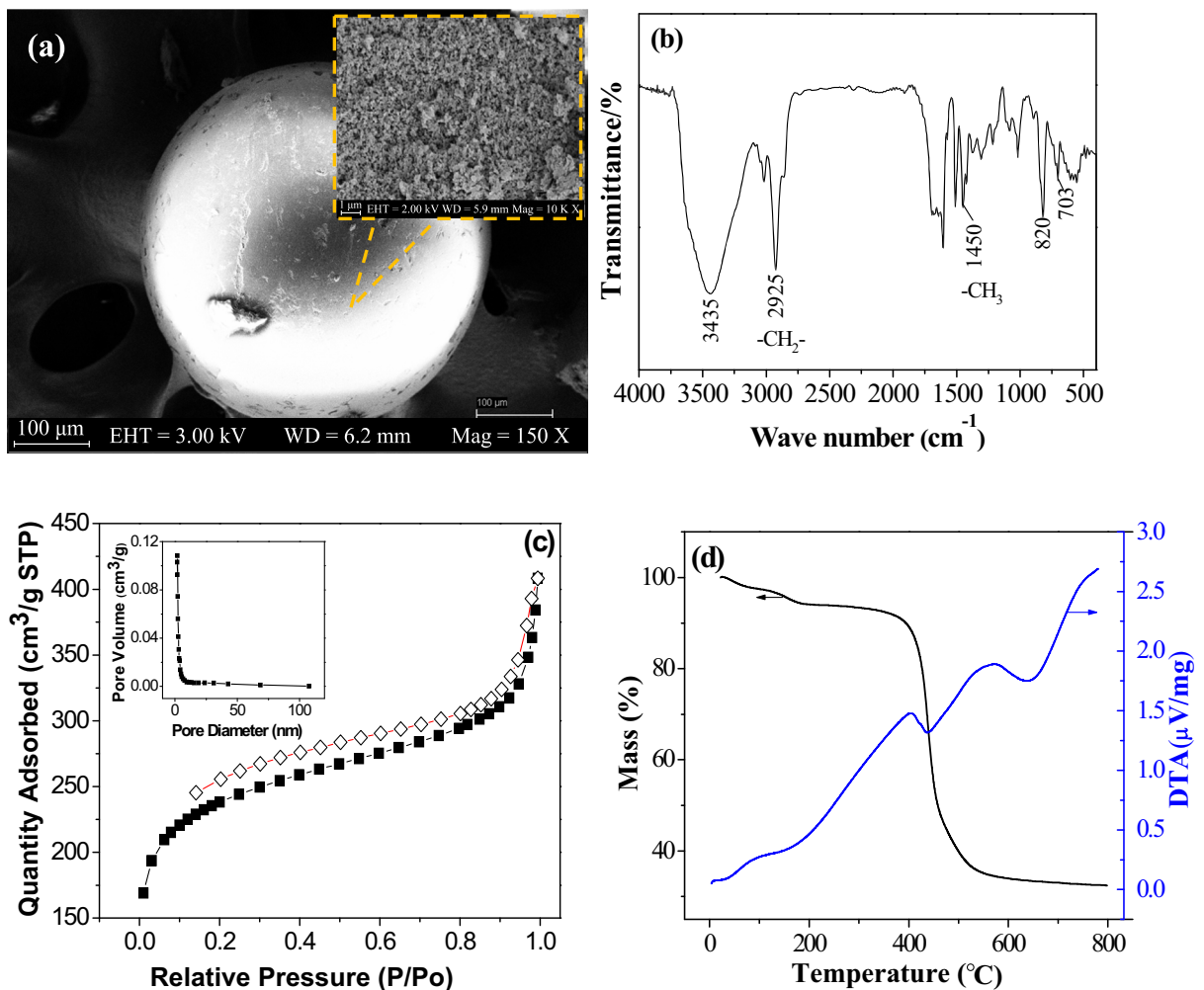


Fig. 1 Characterization of L-493. SEM images with magnification of $\times 10\text{ K}$ and $\times 150$ (a); FTIR spectrum (b); N_2 adsorption–desorption isotherms (c); TGA curves (d)

3.2 Effect of Adsorbent Dosage

The effect of adsorbent dosage on the adsorption of THMs is shown in Fig. 2, adsorption followed the order: $\text{CHBr}_3 \approx \text{CHBr}_2\text{Cl} > \text{CHBrCl}_2 > \text{CHCl}_3$, and the removal efficiency increased with increasing adsorbent dosage due to the availability of more adsorbent surface for adsorption (Yakout 2010). Taking into account efficiency and economy, 1.0 g/L (solid-to-liquid ratio) was chosen as the optimum adsorbent dosage for all subsequent experiments.

3.3 Effect of pH and Ionic Strength

pH had no significant effect on the adsorption of THMs on L-493 in the range 3.0–7.0, and only a small decrease in the range 7.0–9.0 (Fig. 3a). Measurements of the zeta potentials of L-493 (Fig. 3b) show a progressively increasing negative charge over the pH range 3.0–10.0, as reported in previous studies (Lu et al. 2005). The adsorption mechanisms were further investigated by quantum chemistry calculations, which are described in Section 3.8. A pH of 7.0 was chosen for all subsequent experiments, as representative of typical drinking water, and the mechanisms that operate for the adsorption of THMs by L-493 are investigated further in the following sections.

Since appreciable amounts of salts are commonly present in waters, the effect of ionic strength on the

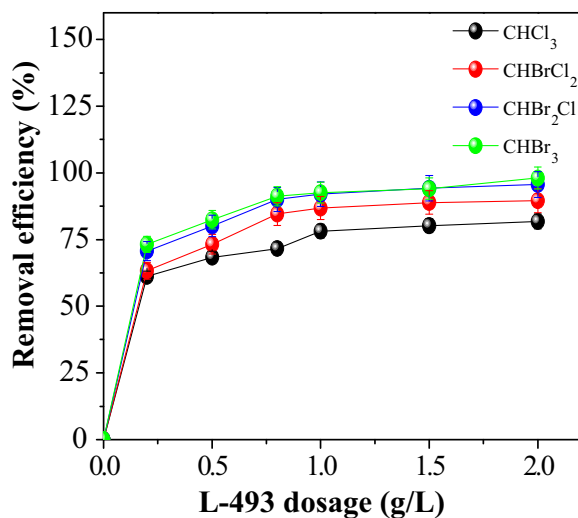


Fig. 2 Effect of adsorbent dosage on the removal efficiencies of THMs adsorption by L-493. Experimental conditions: $[\text{THMs}]_0 = 200 \mu\text{g/L}$, [phosphate buffer] = 5 mM, $I = 1$ mM, contact time = 24 h, pH 7.0, 25 °C

adsorption of THMs on L-493 was studied (Fig. S1). Small decreases in adsorption of THMs occurred when NaCl concentrations were increased from 0 to 30 mM, possibly because of competition between the THMs and electrolyte for adsorption sites on the resins, but overall these results indicate good performance of L-493 for the removal of THMs from waters, even where there is high salinity.

3.4 Effects of Co-existing Anions and HA

Since natural waters generally have complex compositions, we investigated the effects of typical anions (e.g., Cl^- , NO_3^- , CO_3^{2-} , SO_4^{2-} and PO_4^{3-} , as Na^+ salts, 10 mM each) and HA (6 mg/L) on the adsorption of THMs on L-493, these were spiked individually into working solutions containing 200 $\mu\text{g/L}$ THMs and 1.0 g/L L-493, and as shown in Fig. S2, resulted in only small decreases in THMs adsorption. Considering that the concentrations of these anions in the present measurements were much higher than those typically present in drinking waters, it can be concluded that the presence of these anions is unimportant for THMs adsorption on L-493. Furthermore, the presence of HA at a typical concentration found in river water only slightly decreased the removal efficiency of THMs by L-493.

3.5 Adsorption Kinetics

Adsorption of THMs on L-493 (Fig. 4a) showed a rapid initial increase, but then slowed as the system reached equilibrium (after about 24 h). The adsorption kinetics were investigated by fitting the experimental data to pseudo-first-order (Fig. 4b) and pseudo-second-order models (Fig. 4c), which can be written as (Lagergren 1898):

First-order kinetic equation : (3)

$$\lg(q_e - q_t) = \lg q_e - \frac{k_1}{2.303} t$$

Second-order kinetic equation : $\frac{t}{q_t} = \frac{1}{k_2 q_e^2} + \frac{t}{q_e}$ (4)

where q_e and q_t ($\mu\text{g/g}$) are the amounts of THM adsorbed at equilibrium and at time t (h) respectively, k_1 and k_2 (1/h) are the adsorption rate constant for

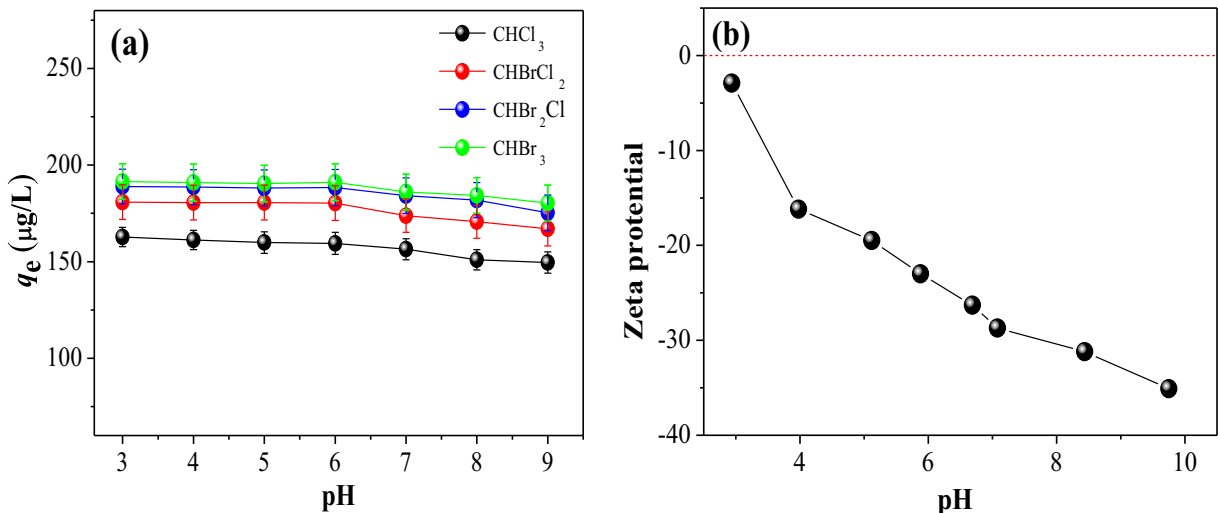


Fig. 3 Effect of pH on the adsorption of THMs on L-493 (a) and zeta-potential of the L-493 (b). Experimental conditions: [L-493 dosage] = 1.0 g/L, [THMs]₀ = 200 $\mu\text{g/L}$, [phosphate buffer] = 5 mM, I = 1 mM, contact time = 24 h, 25 °C

pseudo-first-order reaction and pseudo-second-order reactions ($\text{g}\cdot\mu\text{g}^{-1}\cdot\text{h}^{-1}$), respectively.

The calculated kinetic parameters (Table 1) show that the experimental data are well fitted with the pseudo-second-order model ($R^2 = 0.99$) with calculated q_e that are similar to the experimental values, and thus support the previous report that chemical adsorption is the main adsorption mechanism for L-493 (Ho and McKay 1999).

Since the rate of adsorption of THMs on porous polymeric adsorbents is controlled by a combination of external, interfacial, and internal diffusion, the data were then further analyzed to determine the rate-limiting step.

The intra-particle diffusion equation is as follows (Weber and Morris 1963):

$$q_t = k_{id}t^{0.5} + c_i \quad (5)$$

where k_{id} ($\mu\text{g}\cdot\text{g}^{-1}\cdot\text{h}^{-0.5}$) is the intra-particle diffusion rate constant; c_i is associated with the boundary layer thickness. However, plots of q_t ($\mu\text{g/g}$) versus $t^{0.5}$ (Fig. 4d) were not linear, but could be separated into two linear regions, which indicates that two steps occurred (Table 2). This can be explained as an instantaneous adsorption or external surface adsorption, followed by a gradual adsorption stage where intra-particle diffusion was rate limiting.

3.6 Adsorption Isotherms and Thermodynamic Studies

Adsorption equilibrium isotherms provide important information for elucidating adsorption mechanisms,

and are commonly analyzed by the Langmuir and Freundlich models, which are written as:

Langmuir model (Langmuir 1918) : (5)

$$q_e = \frac{q_m K_L C_e}{1 + K_L C_e}$$

Freundlich model (Freundlich 1906) : (6)

$$q_e = K_F C_e^{\frac{1}{n}}$$

where C_e is the equilibrium concentration of THMs ($\mu\text{g/L}$), q_e is the equilibrium adsorption capacity ($\mu\text{g/g}$), and q_m ($\mu\text{g/g}$) and K_L ($\text{L}/\mu\text{g}$) are the maximum adsorption capacity and Langmuir constant, respectively, and are related to binding sites affinity. K_F ($\mu\text{g/g}$) and n are the Freundlich constants. The parameters calculated from these models are listed in Table S3. As can be seen in Fig. 5, adsorption of THMs is well described by the Langmuir model with high correlation coefficients ($R^2 > 0.99$), and adsorption capacity is in the order CHBr_3 (253.7 $\mu\text{g/g}$) \approx CHBr_2Cl (250.6 $\mu\text{g/g}$) $>$ CHBrCl_2 (247.3 $\mu\text{g/g}$) $>$ CHCl_3 (228.6 $\mu\text{g/g}$). Previously published values for maximum adsorption capacities of THMs on various adsorbents in previous literatures are listed in Table S4 along with those from the present measurements. Although the maximum adsorption capacity of THMs on L-493 is less than that of adsorbents, such as the commercial activated carbon and multiwalled carbon nanotubes (Lu et al. 2005, 2006;

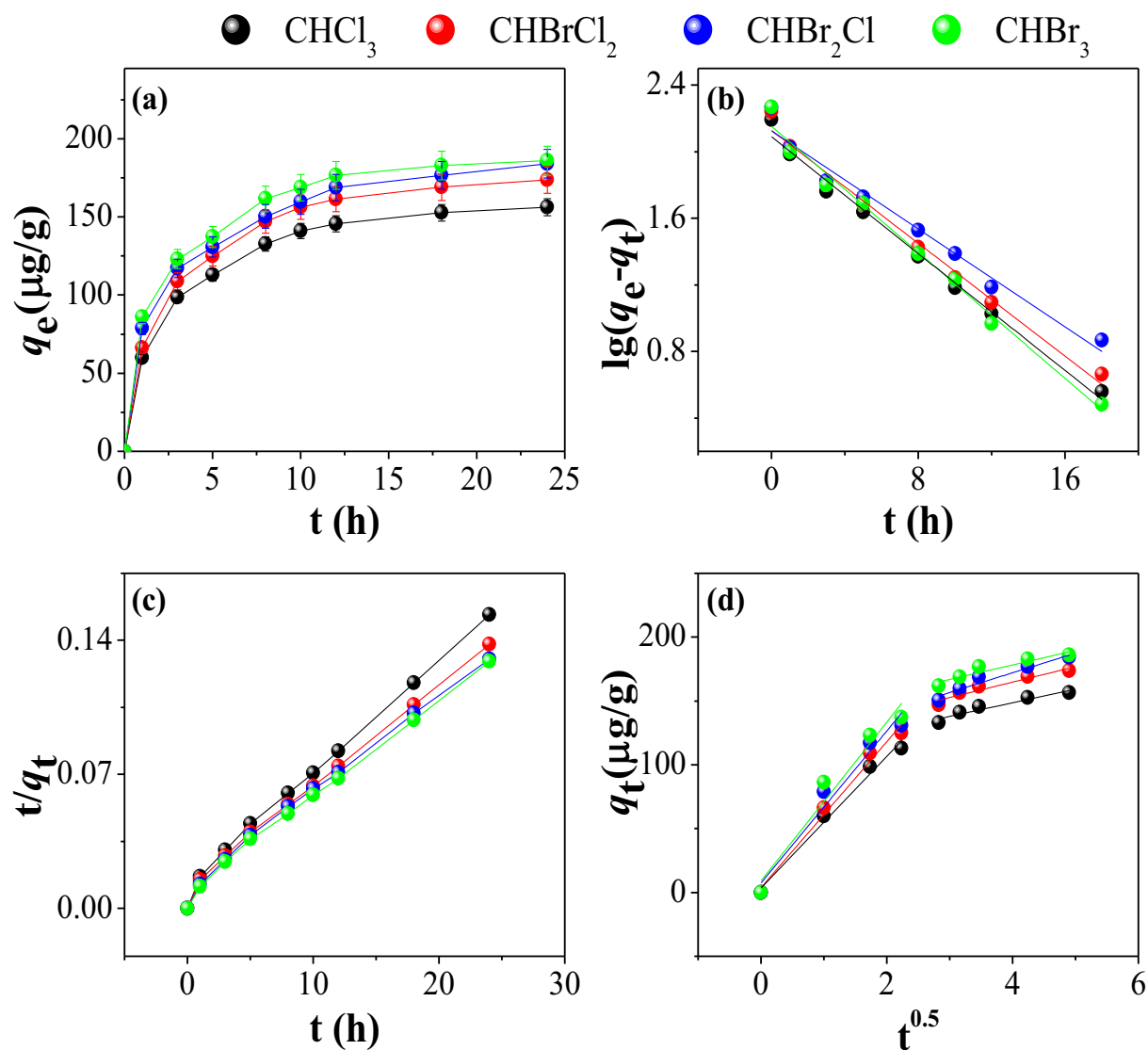


Fig. 4 Effect of contact time on the adsorption of THMs on L-493 (a); fits to kinetic models for adsorption of THMs on L-493 pseudo-first-order (b), pseudo-second-order (c), and intra-particle

diffusion models (d). Experimental conditions: [L-493 dosage] = 1.0 g/L, [THMs]₀ = 200 µg/L, [phosphate buffer] = 5 mM, I = 1 mM, pH 7.0, 25 °C

Tsai et al. 2008), it is similar to that of other resins (Qi et al. 2007).

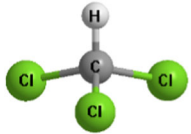

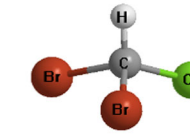
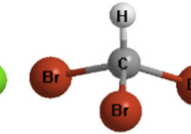
Thermodynamic parameters for THMs adsorption on L-493 were obtained from experiments performed at three different temperatures (15, 25 and 35 °C) (Fig. 5) using the following equations (Eqs. 7–8),

$$\Delta G^\circ = -RT \ln K_d \tag{7}$$

$$\ln K_d = \frac{\Delta S^\circ}{R} - \frac{\Delta H^\circ}{RT} \tag{8}$$

where ΔG° , ΔH° , and ΔS° are the changes in standard Gibbs energy, enthalpy, and entropy of adsorption THMs onto L-493, respectively; K_d is the adsorption distribution coefficient (C_{ads}/C_e), R is the universal gas constant ($8.314 \text{ J}\cdot\text{mol}^{-1}\cdot\text{K}^{-1}$), and T (°C) is the absolute temperature. ΔH° and ΔS° were obtained from the vant Hoff plot of $\ln K_d$ versus $1/T$ (Fig. S3), and the various calculated parameters are summarized in Table S5. The negative values of ΔG° and positive values of ΔH° at all tested temperatures indicate that the adsorption for THMs on L-493 is both spontaneous and endothermic, whilst the

Table 1 Calculated electronic parameters for THMs molecules

Parameter								
		CHCl ₃		CHBrCl ₂		CHBr ₂ Cl		CHBr ₃
Atomic electric potential (atomic units)	C	-14.58	C	-14.59	C	-14.60	C	-14.61
	H	-1.03	H	-1.04	H	-1.04	H	-1.04
	Cl	-64.37	Cl	-64.37	Cl	-64.37	Br	-175.79
	Cl	-64.37	Cl	-64.37	Br	-175.79	Br	-175.79
	Cl	-64.37	Br	-175.79	Br	-175.79	Br	-175.79
Molecular electric potential (atomic units)		-208.72		-320.16		-431.59		-543.02
Dipole moment (debye)	ESP charge	1.37		1.30		1.24		1.13
	Mulliken charge	1.19		1.12		1.05		0.97

values suggest a combination of physisorption and chemisorption. The positive ΔS° values indicate increased

system disorder at the solid–solution interface (Muniyappan Rajiv Gandhi et al. 2010; Mafra et al. 2013).

Table 2 Kinetic parameters for the adsorption of THMs on L-493

Model	Parameter	CHCl ₃	CHBrCl ₂	CHBr ₂ Cl	CHBr ₃
Pseudo-first-order	$q_{e, \text{exp}}$ ($\mu\text{g/g}$)	109.1	173.8	184.2	186.1
	k_1 (h^{-1})	0.20	0.20	0.17	0.22
	$q_{e, \text{cal}}$ ($\mu\text{g/g}$)	85.70	134.23	133.28	142.13
	R^2	0.989	0.986	0.971	0.987
Pseudo-second-order	k_2 ($\text{g}\cdot\mu\text{g}^{-1}\cdot\text{h}^{-1}$)	5.73×10^{-3}	3.56×10^{-3}	3.41×10^{-3}	4.06×10^{-3}
	$q_{e, \text{cal}}$ ($\mu\text{g/g}$)	114.7	182.5	191.2	194.2
	R^2	0.992	0.992	0.991	0.994
	Intra-particle diffusion model	$k_{\text{id},1}$ ($\mu\text{g}\cdot\text{g}^{-1}\cdot\text{h}^{-0.5}$)	36.02	57.17	59.56
$c_{i,1}$		2.61	4.15	7.78	9.43
R^2		0.980	0.980	0.952	0.939
$k_{\text{id},2}$ ($\mu\text{g}\cdot\text{g}^{-1}\cdot\text{h}^{-0.5}$)		7.45	12.08	15.40	11.30
$c_{i,2}$		74.02	116.68	110.75	133.27
R^2		0.898	0.909	0.921	0.864

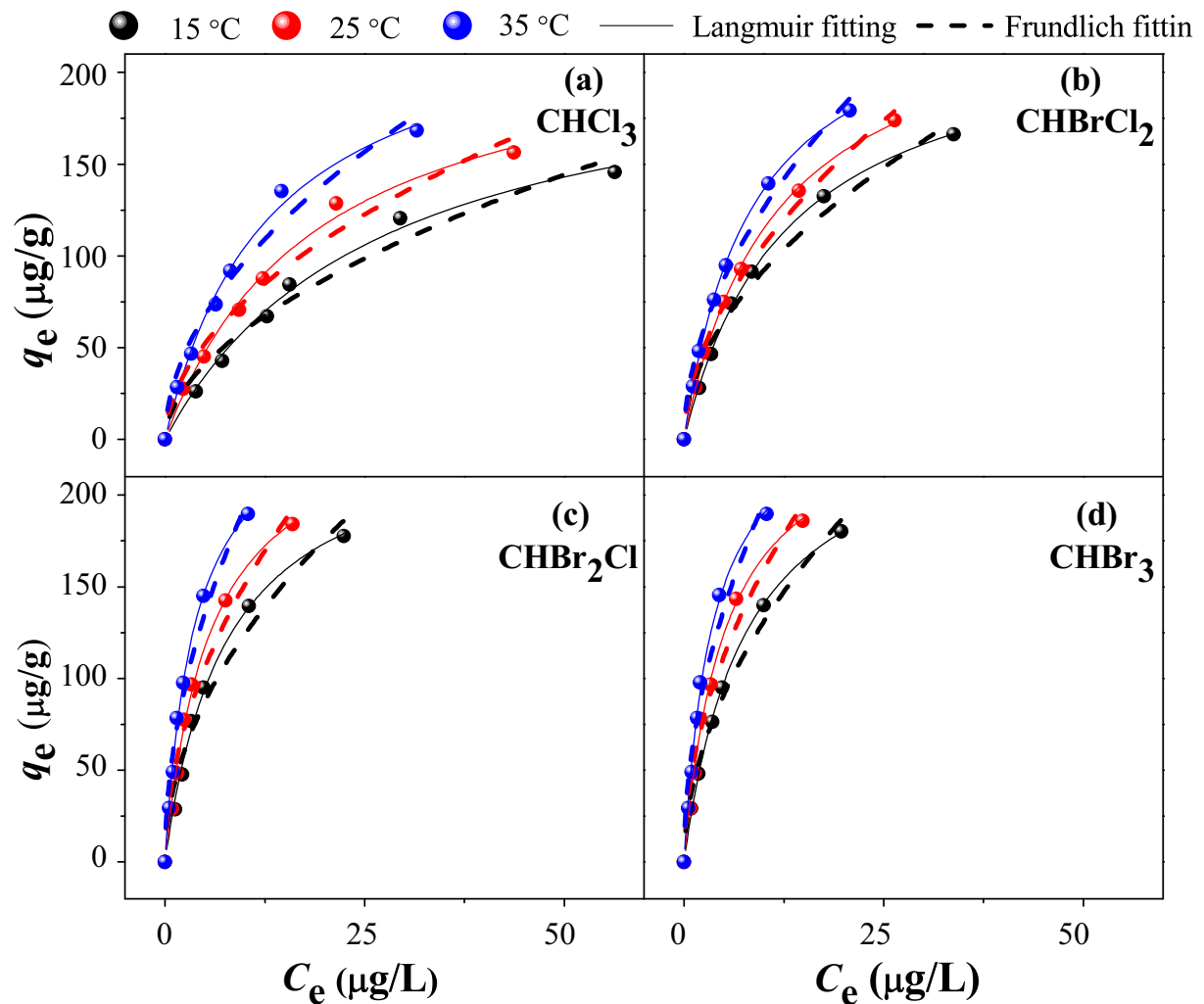


Fig. 5 Isotherms for the adsorption of individual THMs on L-493. Experimental conditions: [L-493 dosage] = 1.0 g/L, [THMs]₀ = 0–200 µg/L, [phosphate buffer] = 5 mM, $I = 1$ mM, contact time = 24 h, pH 7.0

3.7 Selective Adsorption of THMs in Single and Mixed Systems

As shown in Fig. 6, for the single and mixed systems, the adsorption capacities are in the order $\text{CHBr}_3 \approx \text{CHBr}_2\text{Cl} > \text{CHBrCl}_2 > \text{CHCl}_3$. THMs adsorption in the mixed system is the same order as that in single systems. To gain a better understanding of the THMs adsorption process, charge distributions (i.e., Electrostatic Potential (ESP) and Mulliken electronegativity) and dipole moments were calculated for the optimized structures using DFT (Table 2). The higher adsorption capacities of the bromo-THMs compared to chloroform

(Morris and Boyd 1987) can be explained by the increase in their electronic potential and decrease in polarity. There is also a direct relationship between the dipole moments, molecular electronic potential and THM adsorption capacity ($R^2 > 0.98$). If the dipole moment is the main factor determining the adsorption interaction (Fig. S4), it explains the observation of pH having little effect on the adsorption of THMs. For molecular electronic potential, the higher value means a stronger electrostatic interaction, which leads to higher adsorption capacity (Fig. S5). Consequently, both hydrophobic effects and electrostatic interactions play important roles in the adsorption process.

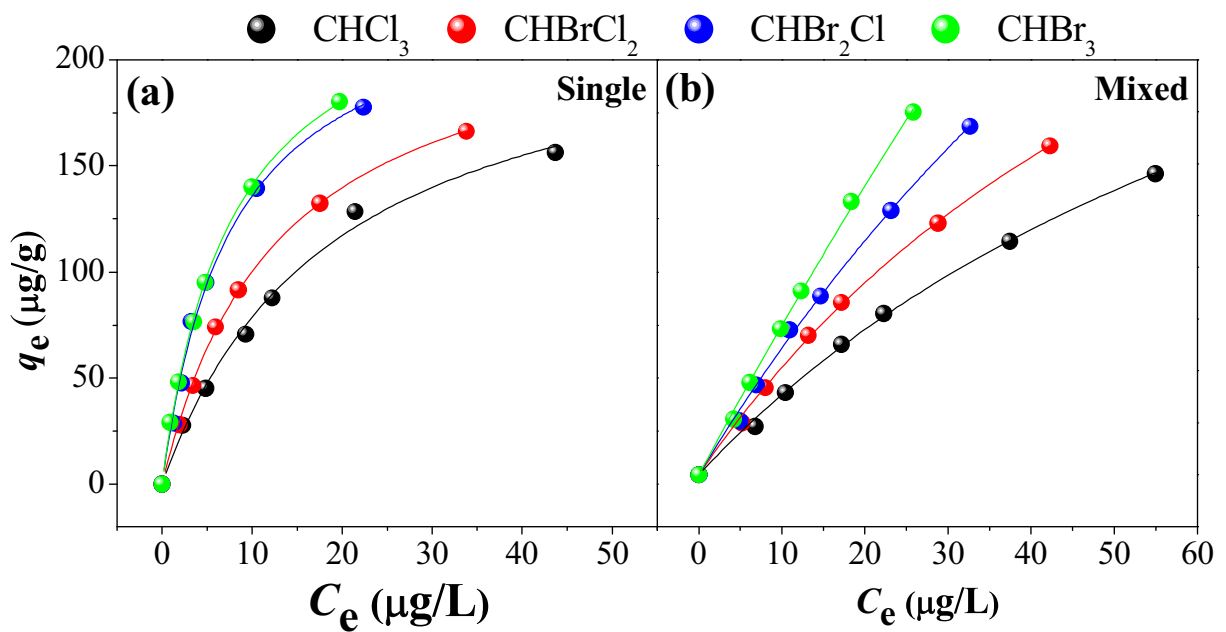


Fig. 6 Selective adsorption of THMs from single and mixed systems containing equimolar amounts of each THM. Experimental conditions: [L-493 dosage] = 1.0 g/L, [THMs]₀ = 0–200 µg/L, [phosphate buffer] = 5 mM, *I* = 1 mM, contact time = 24 h, pH 7.0, 25 °C

3.8 Comparison of Adsorption Properties of L-493 with Those of Various Commercial Adsorbents

Adsorption of THMs on L-493 resin was compared with several other commercial resins (i.e., IRC 748, XAD-4, XAD-1180, IR 120) and powder activated carbon,

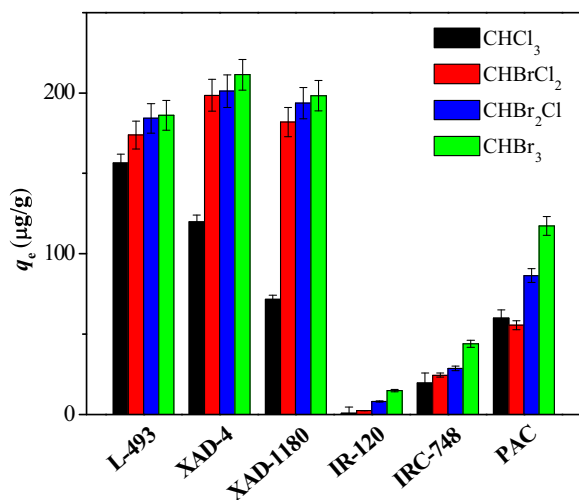


Fig. 7 Comparison of the adsorption properties of L-493 for THMs with those of various commercial resins. Experimental conditions: [L-493 dosage] = 1.0 g/L, [THMs]₀ = 200 µg/L, [phosphate buffer] = 5 mM, *I* = 1 mM, contact time = 24 h, pH 7.0, 25 °C

which are currently used for the removal of THMs from waters. L-493, XAD-4 and XAD-1180 all performed well (Fig. 7), but L-493 showed the highest adsorption capacity for chloroform, and is thus potentially a good adsorbent for the removal of THMs from drinking water. Adsorption capacity is influenced by several factors, including specific surface area, adsorbent polarity, and pore structures. Compared with that of IRC 748 with the

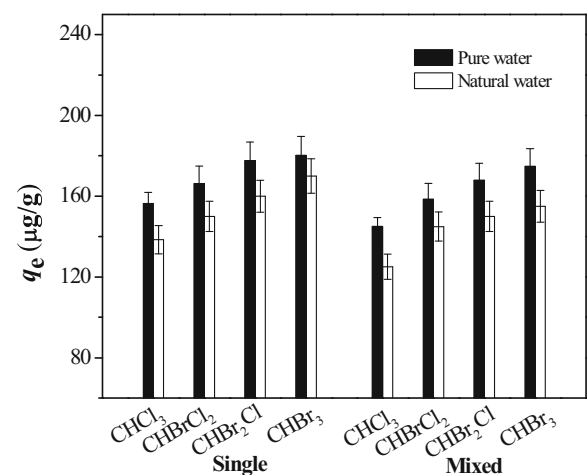


Fig. 8 Effect of a natural water matrix on the adsorption of THMs on L-493. Experimental conditions: [THMs]₀ = 200 µg/L, [L-493 dosage] = 1.0 g/L, pH 7.0, 25 °C

specific surface areas, three resins (e.g., L-493, XAD-4, or XAD-1180) with highest specific surface areas have the highest adsorption capacities for THMs, suggesting that the specific surface area is a major factor for determining the adsorption capacity.

3.9 Desorption and Regeneration

Regeneration of used L-493 was investigated by a bath experiment in a desorption/regeneration study using various desorbing agents; a desorption efficiency of ~98% was observed with a 6-h treatment with 0.1 NaOH. The results of THMs adsorption over 5 adsorption/regeneration with 0.1 M NaOH cycles are shown in Fig. S6. Only small decreases in THM adsorption capacity was observed after 5 cycles, thus indicating that L-493 can be reused multiple times in drinking water treatment without appreciable loss in adsorption performance.

3.10 Application to Natural Waters

We further investigated the practical performance of L-493 by investigating a natural water spiked with THMs. The results for THM adsorption from this natural water by L-493 were only slightly lower than those obtained with pure water (Fig. 8), although there were appreciable differences in adsorption from single and multicomponent systems.

4 Conclusions

This work has systematically investigated the adsorption of THMs from water by a commercial Dowex L-493 resin, with the following conclusions:

- (1) The adsorption capacity of L-493 for THMs increased with the number of Br atoms; overall, it was comparable with the best of the other commercial resins investigated, but it was superior for the adsorption of chloroform.
- (2) Adsorption of THMs on L-493 was well described by the Langmuir model; it was not affected by pH in the range 4.0–7.0, but decreased slightly at higher pH.
- (3) The adsorption process obeyed pseudo-second-order kinetics, and thermodynamic calculations

indicate that it is endothermic and spontaneous for each THM.

- (4) Overall, these results demonstrate that L-493 is potentially a good adsorbent for the removal of THMs from water, especially chloroform.

Acknowledgments This work was financially supported by the National Key Research and Development Program of China (2016YFD0600804), National Natural Science Foundation of China (Grant Nos.: 21367004, 21567004, and 2167005), Guangxi Natural Science Foundation (Grant Nos.: 2016GXNSFCA, 2014GXNSFAA118284, and 14123006-24), and Young Scholar Innovation Team and the Scientific Research Foundation of Guangxi University for Nationalities (2016, YCSW2018121, and 2013MDYB031).

Compliance with Ethical Standards

Conflict of Interest The authors declare that they have no conflict interest.

References

- Babi, K. G., Koumenides, K. M., Nikolaou, A. D., Makri, C. A., Tzoumerkas, F. K., & Lekkas, T. D. (2007). Pilot study of the removal of THMs, HAAs and DOC from drinking water by GAC adsorption. *Desalination*, 210(1–3), 215–224.
- Bull, R. J., Brinbaum, L., Cantor, K. P., Rose, J. B., Butterworth, B. E., Pegram, R., et al. (1995). Water chlorination: Essential process and cancer hazard? *Toxicological Sciences*, 28(2), 155–166.
- Chiang, P. C., Chang, E. E., Chang, P. C., & Huang, C. P. (2009). Effects of pre-ozonation on the removal of THM precursors by coagulation. *Science of the Total Environment*, 407(21), 5735–5742.
- Frendlich, H. M. A. (1906). Concerning adsorption in solutions. *Journal of Physical Chemistry*, 57, 385–470.
- Frisch, M. J., Trucks, G. W. T., Schlegel, H. B., Scuseria, G. E., Robb, M. A., Cheeseman, J. R., et al. (2010). *Gaussian 09, Revision C.01*. Wallingford: Gaussian, Inc..
- Ho, Y. S., & McKay, G. (1999). Pseudo-second order model for sorption processes. *Process Biochemistry*, 34, 451–465.
- Lagergren, S. K. (1898). About the theory of so-called adsorption of soluble substances. *Kungl. Svenska Vetenskapsakademiens Handlingar*, 24, 1–39.
- Langmuir, I. (1918). The adsorption of gases on plane surfaces of glass, mica and platinum. *Journal of the American Chemical Society*, 40(9), 1361–1403.
- Lu, C., Chung, Y. L., & Chang, K. F. (2005). Adsorption of trihalomethanes from water with carbon nanotubes. *Water Research*, 39(6), 1183–1189.
- Lu, C., Chung, Y. L., & Chang, K. F. (2006). Adsorption thermodynamic and kinetic studies of trihalomethanes on

- multiwalled carbon nanotubes. *Journal of Hazardous Materials*, 138(2), 304–310.
- Mafra, M. R., Mafra, L. I., Zuim, D. R., Vasques, É. C., & Ferreira, M. A. (2013). Adsorption of remazol brilliant blue on an orange peel adsorbent. *Brazilian Journal of Chemical Engineering*, 30(3), 657–665.
- Morris, R. B., & Boyd, R. N. (1987). *Organic chemistry*. New York: Allyn & Bacon Inc..
- Muniyappan Rajiv Gandhi, Natrayasamy, V., & Meenakshi, S. (2010). Adsorption mechanism of hexavalent chromium removal using Amberlite IRA 743 resin. *Ion Exchange Letter*, 3, 25–35.
- Pan, B., Zhang, Q., Meng, F., Li, X., Zhang, X., Zheng, J., et al. (2005). Sorption enhancement of aromatic sulfonates onto an aminated hyper-cross-linked polymer. *Environmental Science and Technology*, 39(9), 3308–3313.
- Pan, B., Zhang, W., Pan, B., Qiu, H., Zhang, Q., Zhang, Q., et al. (2008). Efficient removal of aromatic sulfonates from wastewater by a recyclable polymer: 2-naphthalene sulfonate as a representative pollutant. *Environmental Science and Technology*, 42(19), 7411–7416.
- Prarat, P., Ngamcharussrivichai, C., Khaodhiar, S., & Punyapalakul, P. (2011). Adsorption characteristics of haloacetonitriles on functionalized silica-based porous materials in aqueous solution. *Journal of Hazardous Materials*, 192(3), 1210–1218.
- Prarat, P., Ngamcharussrivichai, C., Khaodhiar, S., & Punyapalakul, P. (2013). Removal of haloacetonitriles in aqueous solution through adsorbent modification process by polymerizable surfactant-modified mesoporous silica. *Journal of Hazardous Materials*, 244–245, 151–159.
- Qi, J., Wang, S. X., Yu, X. C., Fei, Z. H., & Zhai, Z. C. (2007). Removal of the by-products from chlorination disinfection in aqueous solution by resin adsorption (in Chinese). *Journal of Jiaxing University*, 19, 62–66.
- Tsai, J. H., Chiang, H. M., Huang, G. Y., & Chiang, H. L. (2008). Adsorption characteristics of acetone, chloroform and acetonitrile on sludge-derived adsorbent, commercial granular activated carbon and activated carbon fibers. *Journal of Hazardous Materials*, 154(1–3), 1183–1191.
- USEPA. (1998). National primary drinking water regulations: Disinfectants and disinfection byproducts, Final rule. *Federal Register*, 63(241), 69390–69476.
- USEPA Method 551.1 (1990). Determination of chlorination disinfection byproducts, chlorinated solvents, and halogenated pesticides/herbicides in drinking water by liquid–liquid extraction and gas chromatography with electroncapture detection. Office of Research and Development, U.S. Environmental Protection Agency, Cincinnati, OHIO.
- Uyak, V., Koyuncu, I., Oktem, I., Cakmakci, M., & Toroz, I. (2008). Removal of trihalomethanes from drinking water by nanofiltration membranes. *Journal of Hazardous Materials*, 152(2), 789–794.
- Wang, Q., Shi, P., Ma, Y., Li, A., Wang, J., Ma, R., et al. (2014). The performance of quaternized magnetic microspheres on control of disinfection by-products and toxicity in drinking water. *Chemical Engineering Journal*, 254, 230–236.
- Weber, W. J., & Morris, J. C. (1963). Kinetics of adsorption on carbon from solution. *Journal of the Sanitary Engineering Division, American Society of Civil Engineers*, 89(2), 31–60.
- Wegmann, C., Suárez García, E., & Kerkhof, P. J. A. M. (2011). Kinetics of acrylonitrile adsorption from an aqueous solution using Dowex Optipore L-493. *Separation and Purification Technology*, 81(3), 429–434.
- Yakout, S. M. (2010). Removal of trihalomethanes from aqueous solution through adsorption and photodegradation. *Adsorption Science and Technology*, 28(7), 601–610.
- Yıldız, O., Citak, D., Tuzen, M., & Soylak, M. (2011). Determination of copper, lead and iron in water and food samples after column solid phase extraction using 1-phenylthiosemicarbazide on Dowex Optipore L-493 resin. *Food and Chemistry Toxicology*, 49(2), 458–463.